Prediction of Radiated Fields from Cable Bundles based on Current Distribution Measurements

Jin Jia, Denis Rinas, Stephan Frei
Technische Universität Dortmund
Dortmund, Germany
jin.jia@tu-dortmund.de
denis.rinas@tu-dortmund.de
stephan.frei@tu-dortmund.de

Abstract— **In automotive EMC ALSE method, specified in CISPR 25, is commonly used for emission measurements. Components or modules are required to be connected with a test cable bundle for evaluating radiated emissions. The radiation is often mainly dominated by the common mode current along the cable bundle. In order to predict radiated emissions from setups according to ALSE method, without using a large anechoic chamber, this paper presents an alternative and innovative method. The presented approach determines radiated fields from a cable bundle without phase information. It is only based on the amplitude of common mode current from phaseless measurements using a RF current probe. Firstly, radiation model of a cable bundle is simplified to a single equivalent transmission line (TL) according to the mode analysis of multiconductor transmission line (MTL) theory. Then an optimization procedure based on *trust-region-reflective* (TRR) method and *multi-start point* algorithm is used to determine the common mode parameters of the equivalent TL by fitting to the measured current amplitude. The phase of common mode current, therefore, is retrieved through optimized TL parameters. Finally, the radiated fields are straightforwardly evaluated by elementary dipoles approximation of the cable bundle. The proposed approach is verified by numerical analysis of different cable bundle models and measurements. The stability and feasibility to evaluate radiated emissions from a cable bundle could be shown.**

Keywords- Automotive EMC; CISPR 25; radiated emissions; cable bundle; common mode current; MTL;mode analysis

I. INTRODUCTION

Radiated emissions measurements from electronic components or modules connected to a cable bundle require an anechoic shielded chamber to eliminate extraneous disturbance and avoid wall reflections. In automotive EMC the ALSE method from CISPR 25 [1] is commonly used. Due to high costs and space consumption of anechoic chambers it is desirable to find better methods, at least for pre-compliance measurements. Because a strong correlation between common mode current along a cable bundle connecting to EUT and the measured radiated emissions [2] exists, common mode current measurements can be an alternative for evaluating radiated emissions. The RF current probes combined with a spectrum analyzer can be used to measure current amplitude distribution along cable bundles. In order to calculate the radiated far-fields, the spatial current amplitude distribution is not enough. The phase is needed, and this is a bottle-neck for predicting radiated emissions from cable bundles.

There are three solutions proposed for the phaseless field prediction in recent publications. The first solution [2] is based on transfer function integrating measurement environment influence. The phase information is approximated from a signum function that imparts either a relative 0˚ phase shift or 180˚ phase shift, according to electrical length of cable at the measured frequency. This method is suitable for simple models in low frequency, but difficult to deal with more practical applications, for example complex cable bundles radiating at high frequencies. The second proposal aims at measuring phase straightforwardly mainly in application of radiation modeling from near field scanning measurements. Time domain measurements [3] can receive amplitude and phase of field simultaneously through FFT. However the data noise from environment is a big challenge for reliability and effectiveness of this approach. Additionally phase measurements in frequency domain [4] are demanding in terms of instruments and measurement accuracy. The last approach [5] is based on the use of phaseless measurement. It retrieves the full complex field distribution, only from the knowledge of near-field amplitude data through special phase retrieval algorithms for solving an inverse problem. But the main challenge for this approach is to find the global minimum.

Compared to a complicate electronic printed circuit board, the radiation characteristics from even complex cable bundles are simpler and more regular. Therefore current amplitude measurements from cable bundles, combined with specific phase retrieval algorithms and equivalent dipoles method, is sufficient to predict radiated emissions. In this work a system for measurements of common mode current amplitude distribution, as shown in figure 1 and comprising a RF current probe and a stepper motor, is used for predicting the far-fields form cable bundles. A phase retrieval algorithm was developed which is based on MTL mode analysis theory (section II). In section III, a new optimization procedure for phase retrieval is introduced, including an objective function and a parameter optimization algorithm. Furthermore the main measurement and data processing work flow is explained. The proposed method was verified by measurements and numeric simulations of a twisted pair cable driven by common mode

and differential voltage source respectively and a more complex bundle with 7 wires. Results are presented in section IV. Final section summarizes and discusses the proposed approach.

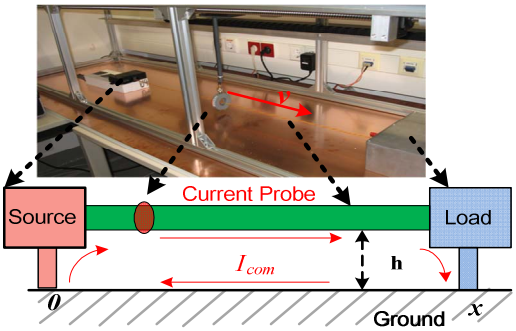

Figure 1. The measurement system for common mode current amplitude distribution of a cable bundle

II. RADIATION MODEL FOR A CABLE BUNDLE

According to mode theory of multiconductor transmission lines [6], MTL can be decoupled to a set of single transmission lines with different properties (propagation constant and characteristic impedance). Figure 2 shows N wires with a per-unit-length impedance matrix $[\boldsymbol{Z}]$ and admittance matrix $[\boldsymbol{Y}]$. $[V_S]$ is the voltage source matrix; $[\boldsymbol{Z}_S]$ and $[\boldsymbol{Z}_L]$ are matrices characterizing the impedance networks connected to the cable bundle extremities.

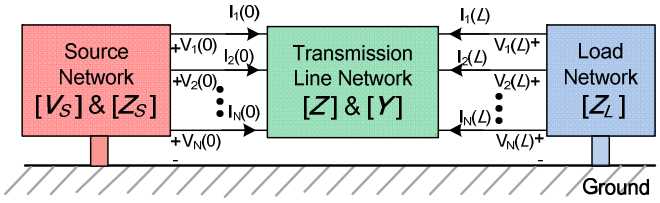

Figure 2. Multiconductor transmission line network

In implementing this mode analysis method, the actual line current $[\boldsymbol{I}]$ and voltage $[\boldsymbol{V}]$ can be expressed by mode quantities $[\boldsymbol{i}_m]$ and $[\boldsymbol{v}_m]$ through decoupling transformation:

$$[\boldsymbol{I}]=[\boldsymbol{T}_i][\boldsymbol{i}_m] \quad [\boldsymbol{V}]=[\boldsymbol{T}_v][\boldsymbol{v}_m] \tag{1}$$

Where $[\boldsymbol{T}_i]$ and $[\boldsymbol{T}_v]$ are formed by the eigenvectors of the product matrices $[\boldsymbol{Y}][\boldsymbol{Z}]$ and $[\boldsymbol{Z}][\boldsymbol{Y}]$ respectively. Based on these two transformation matrices, we can calculate mode voltage source and mode termination impedance matrices:

$$[\boldsymbol{V}_{Sm}]=[\boldsymbol{T}_v]^{-1}[\boldsymbol{V}_S] \tag{2}$$

$$[\boldsymbol{Z}_{S(L)m}]=[\boldsymbol{T}_v]^{-1}[\boldsymbol{Z}_{S(L)}][\boldsymbol{T}_i] \tag{3}$$

The current of common mode component, propagating between cable bundle and the ground plane which dominates radiated emissions, possesses the largest propagation mode velocity compared to other differential modes [7]. Thereby MTL mode propagation constant matrix $[\boldsymbol{\gamma}_m]$ and mode characteristic impedance matrix $[\boldsymbol{Z}_{Cm}]$ can be approximated as combination of common mode component (γ_{com}, Z_{com}) and other differential modes components (γ_d, Z_d) respectively, as described in (4) and (5).

$$[\boldsymbol{\gamma}_m]=\sqrt{[\boldsymbol{T}_v]^{-1}([\boldsymbol{Z}][\boldsymbol{Y}])[\boldsymbol{T}_v]}=\begin{bmatrix}\gamma_{com} & 0 & \cdots & 0\\ 0 & \gamma_{d1} & \ddots & \vdots\\ \vdots & \ddots & \ddots & 0\\ 0 & \cdots & 0 & \gamma_{d(N-1)}\end{bmatrix} \tag{4}$$

$$[\boldsymbol{Z}_{Cm}]=[\boldsymbol{T}_v]^{-1}([\boldsymbol{Z}][\boldsymbol{T}_i][\boldsymbol{\gamma}_m]^{-1}[\boldsymbol{T}_i]^{-1})[\boldsymbol{T}_i]$$
$$=\begin{bmatrix}Z_{com} & 0 & \cdots & 0\\ 0 & Z_{d1} & \ddots & \vdots\\ \vdots & \ddots & \ddots & 0\\ 0 & \cdots & 0 & Z_{d(N-1)}\end{bmatrix} \tag{5}$$

Furthermore due to a cable bundle commonly carrying tightly packed insulated wires, it is reasonable to neglect the contribution of differential mode currents to radiated emissions. Therefore the radiation model for a cable bundle of common mode current can be simplified, as shown in figure 3. A similar common mode model for a cable bundle is presented in [8]. However it is applied for susceptibility testing for cable bundles with double bulk current injection.

According to TL theory, the common mode current at an arbitrary point $I_{com(x)}$ can be expressed by:

$$I_{com(x)}=\left(\frac{e^{\gamma_{com}(L-x)}}{1-\Gamma_2}\right)\left(1-\Gamma_2 e^{-2\gamma_{com}(L-x)}\right)I_{com(L)} \tag{6}$$

Where $I_{com(L)}$ is the current at the cable end; Γ_2 is the load reflection coefficient; γ_{com} is the common mode propagation constant of the cable bundle. Γ_2 and γ_{com} are defined by:

$$\Gamma_2=\frac{Z_{com\_load}-Z_{com}}{Z_{com\_load}+Z_{com}}=A+iB \tag{7}$$

$$\gamma_{com}=\alpha+i\beta \tag{8}$$

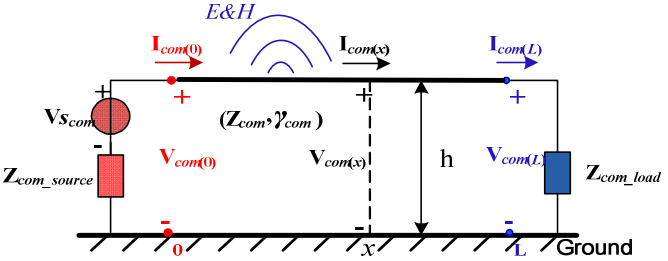

Figure 3. The common mode current radiation equivalent model for a cable bundle

From (6) – (8) except position coordinate x, common mode current $I_{com(x)}$ is a function of the transmission line parameters A, B, α, and β. The parameters here are also the functions of frequency.

III. PHASE RETRIEVAL BASED ON COMMON MODE CURRENT AMPLITUDE MEASUREMENTS

As discussed in section I, the phase information of the common mode current is indispensable to predict radiated emissions from a cable bundle. Determination of phase based on amplitude measurements is an inverse problem. It means TL parameters A, B, α, and β in (6) must be found through appropriate fitting algorithms.

A. *The objective function of the problem*

For avoiding highly nonlinear computations in objective function, we define with (6) a quadratic normalized function:

$$\boldsymbol{F}(x)=\left|\frac{I_{com(x)}}{I_{com(L)}}\right|^2=\left|\left(\frac{e^{\gamma_{com}(L-x)}}{1-\Gamma_2}\right)\left(1-\Gamma_2 e^{-2\gamma_{com}(L-x)}\right)\right|^2 \tag{9}$$

Substituting (7) and (8) into (9), $\boldsymbol{F}(x)$ can also be expressed with respect to A, B, α, and β:

$$\boldsymbol{F}(x)=\frac{e^{-2\alpha(x-L)}}{(1-A)^2+B^2}\left\{\begin{aligned}&\left[1-Ae^{2\alpha(x-L)}\cos(2\alpha(x-L)\beta)+Be^{2\alpha(x-L)}\sin(2\alpha(x-L)\beta)\right]^2\\&+\left[Ae^{2\alpha(x-L)}\sin(2\alpha(x-L)\beta)+Be^{2\alpha(x-L)}\cos(2\alpha(x-L)\beta)\right]^2\end{aligned}\right\} \tag{10}$$

$\boldsymbol{F}(x)$ is a nonlinear function, where position coordinate along cable bundle x is known but transmission line parameters A, B, α, and β have to be found. From measured data at scanning points more equations than unknowns (A, B, α, and β) can be formulated. For the overdetermined equation system a feasible solution set can be found. Therefore this system needs a suitable optimization method to find the best approximate solution for the unknowns. In this work the TRR iterative algorithm [9] was employed to find common mode transmission line characteristics and the current distribution. This algorithm is able to find transmission line parameters A, B, α, and β so that the sum of squares of deviation $S(P)$ is minimal, for a given set of measurements points $\boldsymbol{F}_{meas}(x)$. The objective function $S(P)$ can be expressed:

$$\begin{aligned}S(P)&=min\left\|\boldsymbol{F}(\alpha,\beta,A,B,x)-\boldsymbol{F}_{meas}(x)\right\|_2^2\\&=\sum_{i=0}^{m}\left[\boldsymbol{F}(\alpha,\beta,A,B,x_i)-\boldsymbol{F}_{meas}(x_i)\right]^2\end{aligned} \tag{11}$$

B. *Parameters optimization*

1) Boundary condition for unknown parameters: In order to search optimization parameters A, B, α, and β with high efficiency, integrating appropriate bounday condition into the TRR algorithm is necessary. The characteristic impedance Z_{com}, mainly determined by common mode capacitance and inductance of cable bundle, can be approximated as a real constant at each frequency point. Thereby load reflection coefficient Γ_2 in (7) can be rewritten by:

$$\Gamma_2=\frac{Z_{com\_load}-Z_{com}}{Z_{com\_load}+Z_{com}}=\frac{[\mathrm{Re}(Z_{com\_load})-Z_{com}]+j[Imag(Z_{com\_load})]}{[\mathrm{Re}(Z_{com\_load})+Z_{com}]+j[Imag(Z_{com\_load})]} \tag{12}$$

Define $Re(Z_{com\_load}) = Re$ and $Imag(Z_{com\_load}) = Im$, we obtain:

$$\begin{aligned}limA&=lim\frac{Re^2+Im^2-Z_{com}^2}{Re^2+Im^2+Z_{com}^2+2ReZ_{com}}=[-1,1]\\limB&=lim\frac{2Im^2Z_{com}}{Re^2+Im^2+Z_{com}^2+2ReZ_{com}}=(-\infty,+\infty)\end{aligned} \tag{13}$$

Further the propagation constant γ_{com} in (8) can also be approximately expressed by:

$$\gamma_{com}=\alpha+j\beta=\frac{R_{DC}}{2Z_{com}}+j\frac{\omega}{v_{com}} \tag{14}$$

ω is angular frequency and v_{com} is common mode propagation velocity. R_{DC} is DC resistance of cables. An accurate resistance formulation should consider skin effect. However, the attenuation has nearly no influence on phase accuracy, due to this reason more accurate formulations for skin effect are not taken into account in this work. So boundaries for γ_{com} can be derived:

$$\begin{aligned}lim\alpha&=[0,1]\\lim\beta&=[\frac{\omega}{2\times10^8},\frac{\omega}{3\times10^8}],\omega=2\pi f\end{aligned} \tag{15}$$

The upper boundary of α is reasonable, because in typical applications R_{DC} is usually much smaller than Z_{com}. The v_{com} is bounded by upper limitation with light velocity in vacuum, but of which lower boundary depends on insulation material around cable bundle and the height of it to ground. In this work we confined the lower boundary of velocity to 2/3 times of light velocity in vacuum.

2) Selection of scanning points: The more input values are available, the higher can be the accuracy of the solution. But due to the limitation from dimension of current probe and scanning efficiency, it is not advisable to scan too many points. Therefore interval of scanning coordinate x should be determined according to equation $\Delta x = \lambda_{min}/10$ and then further subdivided through numeric interpolation algorithm, for example the *Spline* function adopted in this work.

3) Initial parameter set $P_0(A_0, B_0, \alpha_0, \beta_0)$: The key problem in optimzation algorithm is the local minimum phenomenon, that is a point where the function value is smaller than or equal to the value at nearby points but greater than at a more distant point. However a reliable solution of an inverse problem is to search a global minumum point. The initial point $P_0(A_0, B_0, \alpha_0, \beta_0)$ plays a significant role for finding the minimum parameters. A *Multi-start point* algorithm [9] was used, which generates random initial points in boundaries and solves objective function at each initial point. Finally it compares local minimum values of different initial points to achieve the most promising parameters for global minimum search.

C. *Modeling radiated emissions from a cable bbundle*

After the optimized parameters sets $[A_f, B_f, \alpha_f, \beta_f]$ at each frequency are available, the phase at x along the cable bundle can be retrieved ($I_{com}(L)$ gives reference phase):

$$phase\left[\frac{I_{com(x)}}{I_{com(L)}}\right]=phase\left[\left(\frac{e^{\gamma_{com}(L-x)}}{1-\Gamma_2}\right)\left(1-\Gamma_2 e^{-2\gamma_{com}(L-x)}\right)\right] \tag{16}$$

Combining the above retrieved phase with the measured amplitude of common mode current along the cable bundle, the electromagnetic field in any point can be calculated by a multiple-dipole method (MDM), as shown in figure 4.

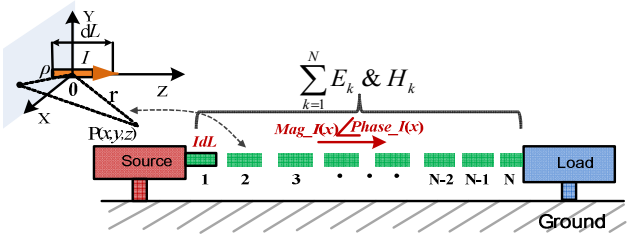

Figure 4. The multiple-dipole model for a cable bundle

The following set of equations defines the radiated magnetic and electric field from a single elementary dipole (only *x*-component is presented):

$$H_x(\omega)=\frac{-IdL\cdot y}{4\pi r}\beta_0^2\left(j\frac{1}{\beta_0 r}+\frac{1}{\beta_0^2 r^2}\right)e^{-j\beta_0 r} \quad (17)$$

$$E_x(\omega)=\frac{IdL\cdot zx}{4\pi r^2}\eta_0\beta_0^2\left(j\frac{1}{\beta_0 r}+\frac{3}{\beta_0^2 r^2}-j\frac{3}{\beta_0^3 r^3}\right)e^{-j\beta_0 r} \quad (18)$$

Where r is the distance from one dipole to the observation point P; ε_0 is dielectric constant of vacuum; dL is Hertzian dipole length; I is the current on a dipole; η_0 is wave impedance in vacuum ($\eta_0=\sqrt{\mu_0/\varepsilon_0}$), where μ_0 is permeability of vacuum. β_0 is the electromagnetic wave phase constant in vacuum. Additionally the influence from ground can be modeled by considering mirror currents in final radiation field calculation [10]. The whole solution procedure can be seen in flow chart in figure 5.

IV. MODEL VALIDATION

A. A twisted pair cable driven by common mode voltage

In order to verify the proposed method, we firstly investigate radiations from a twisted pair cable driven in common mode with Vector Network Analyzer (Agilent, E5061A). The cable is terminated with a 50Ω load. The experiment setup and coordinate system are shown in figure 6.

According to geometry of twisted pair cable and the configuration shown in figure 6, we calculated S21 using antenna voltage V_{ant} and source voltage V_S through Method of Moment (MoM). Figure 7 shows the results of S21 by measurement and MoM. The two curves match very well from 10 MHz up to 1 GHz. Measurement curve below 10 MHz includes obviously noisy data due to the weak capacitive coupling at low frequencies between tested cable and rod antenna. We used RF current probe (FCC, F-65) to scan the common mode current at x = [0:0.06:1.5], and then employed *spline* function to interpolate measured data at x = [0:0.01:1.5]. Both the amplitude and phase of common mode current along the test cable were measured by Vector Network Analyzer to validate the calculated phase by proposed method. Figure 8 depicts current phase variation along the cable bundle at frequencies of 100 MHz and 500 MHz. In these curves, solid lines are measurements and dashed lines are results calculated by phase retrieved algorithm of current amplitude scanning method (CASM) shown in process flow chart of the figure 5.

Compared to the measurements, the CASM can retrieve common mode current phase information along cable with high accuracy. Furthermore we also evaluated electrical field in y-direction at observation point (x = 0.75 m, y = 0 m, z = 0.3 m). Figure 9 shows field values from 30 MHz to 1 GHz by measurement, MoM and proposed CASM. Here the measured E_{y_meas} is obtained according to:

$$E_{y\_meas}=V_{ant\_meas}\times AF_{MoM}$$
$$V_{ant\_meas}=\frac{S21_{meas}\times V_S}{2}\ (V_S=1) \quad (19)$$

The antenna factor AF_{MoM} is calculated by simulation from a verified MoM model in figure 7. V_{ant_meas} is the received

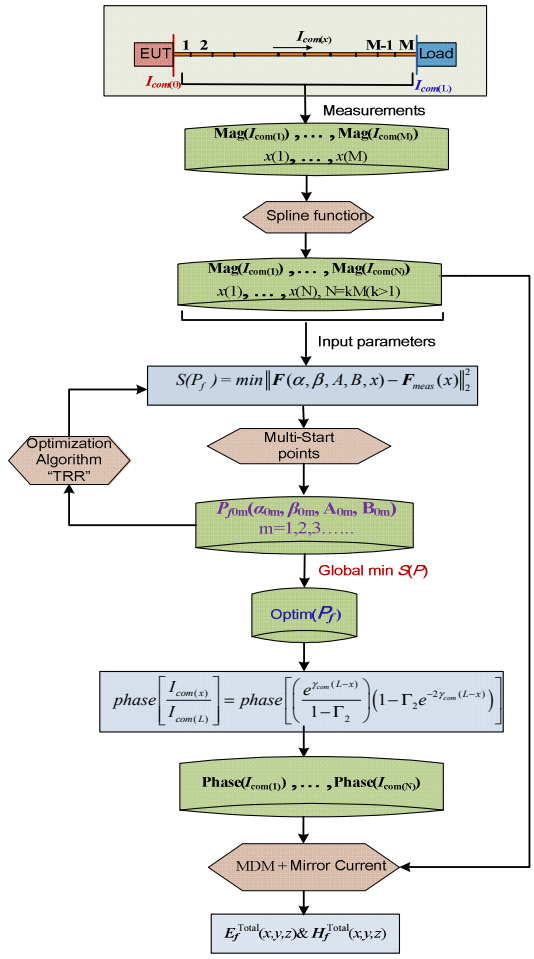

Figure 5. The flow chart of proposed solution algorithm

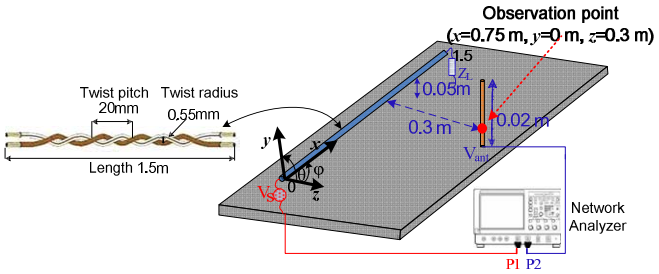

Figure 6. The experiment configuration of twisted pair cable radiation

voltage of rod antenna, calculated by measured S21. The results of proposed CASM match well with measurement and MoM data. However phase retrieved from the measured current amplitude I_{Meas} results in electric field deviation near some resonance frequency points (figure 9), mainly originating from the position inaccuracy when scanning the cable bundle. Another problem in low frequency range (1 MHz – 30 MHz) can be seen in figure 10. In this frequency range the CASM fails to retrieve the correct phase. In order to analyze this problem the fields were computed also with constant phase. This can be done, because the shortest wavelength in low frequency range (10 m at 30 MHz) is about 6 times longer than the length of measured cable (1.5 m). Therefore the phase along the cable can be approximated by a

constant. Compared to CASM, the accuracy is much higher (figure 10). But deviation still exists, that might be due to the inaccurate measured current amplitude. Figure 11 shows the measured function ***F***(x) in (9) compared to MoM results at the frequencies of 1 MHz and 10 MHz along the cable. Deviation can be seen. Therefore if using current amplitude I_{MoM} without measured current amplitude error, CASM can retrieve phase information and predict radiated fields in whole frequency band (1 MHz to 1 GHz) accurately.

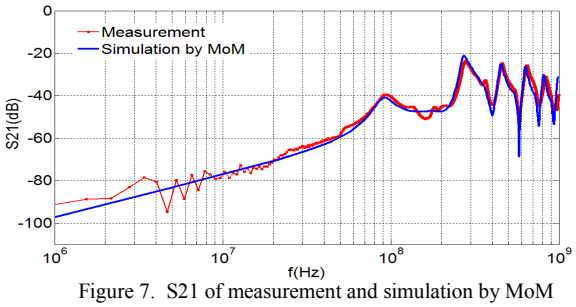

Figure 7. S21 of measurement and simulation by MoM

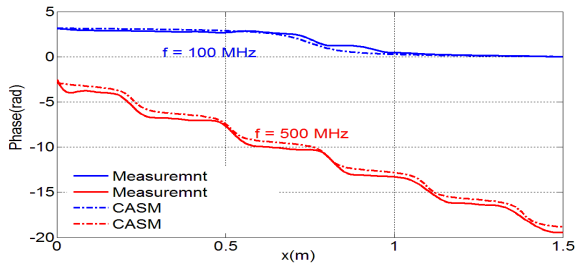

Figure 8. Phase of common current at 100 MHz and 500 MHz of the measurement and CASM

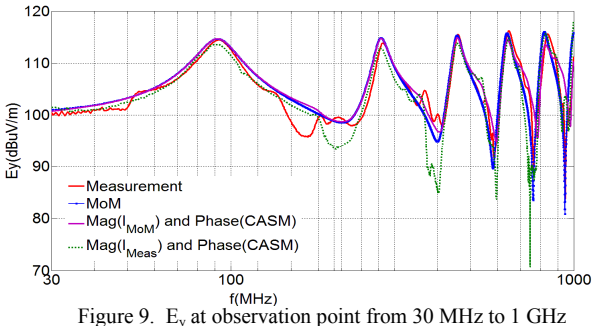

Figure 9. E_v at observation point from 30 MHz to 1 GHz

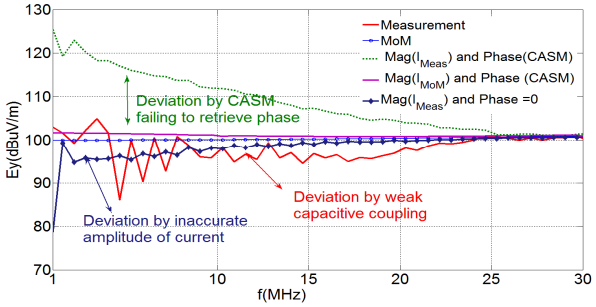

Figure 10. E_y at observation point from 1 MHz to 30 MHz

B. A cable bundle with seven wires

The proposed CASM algorithm was also applied to a 1.5 m long bundle composed of 7 cables. The average height of the bundle is approximately 2 cm above ground plate.

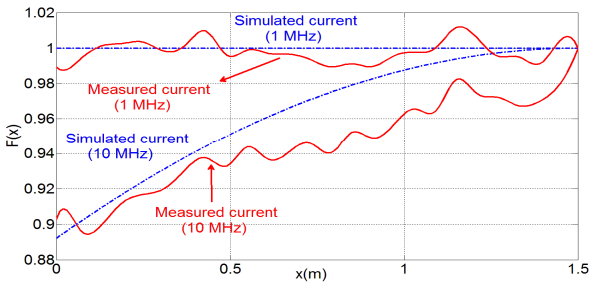

Figure 11. ***F***(*x*) of common mode current for 1 MHz and 10 MHz

The detailed geometry of 2D cross section of the bundle and the experiment setup are shown in figure 12. The simulation model of MoM is the same as for configuration in figure 6 except the twisted pair cable is now represented by seven-cable bundle. The cables in bundle are terminated randomly with resistors, as summarized in Table I.

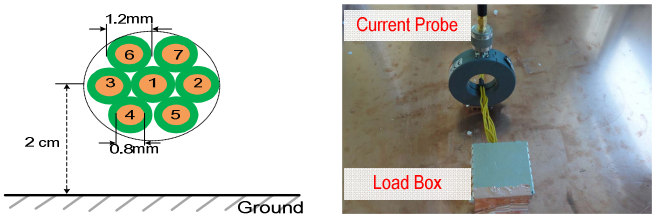

Figure 12. Cross-sectional view and experiment setup for load extremity of the cable bundle

TABLE I. TERMINATION OF THE BUNDLE

	Source Box	**Load Box**
Cable 1 to GND	Feeding(50 Ω)	47 Ω or 10 MΩ
Cable 2 to GND	47 Ω	100 Ω
Cable 3 to GND	100 Ω	47 Ω
Cable 4 to GND	10 Ω	15 kΩ
Cable 5 to GND	15 kΩ	10 Ω
Cable 6 to GND	47 Ω	100 kΩ
Cable 7 to GND	1 kΩ	47 Ω

We investigated two cases of termination resistance for the fed cable; low resistance (47 Ω) and a high resistance (10 MΩ) respectively. In MoM model the cable bundle was divided into 100 segments, and the common mode current along every segment is the sum of currents from the 7 cables in this segment. Only based on amplitude of the common mode current from MoM data, CASM can retrieve phase information of each segment accurately, and further evaluate the electric fields combining with multiple-dipole method and mirror theory. Figure 13 shows electric field in y-direction at the observation point. In addition to the near field, the far-field radiation patterns ($0^\circ \leq \theta \leq 180^\circ$) on the plane $\varphi=0^\circ$ was also calculated using CASM data. Figure 14 shows the electric field in φ- and θ-direction with distance R = 10 m at 900 MHz (only low-load case present). Compared to MoM it is obvious that the proposed CASM can predict near field and far-field

radiation pattern accurately.

Beside the phase was retrieved based on current amplitude of MoM data, we also calculated phase by CASM from measured current amplitude. Figure 15 shows the y-directional electric field at observation point of the fed cable with a low and high load. The solid curve was calculated straightforwardly by the measured amplitude and phase of common mode current. But the dashed curve was calculated by measured current amplitude and the retrieved phase by CASM from this measured current amplitude. The phase from CASM can match with measured data well, except in low frequency range (10 MHz to 30 MHz). This deviation could be caused by current amplitude measurement errors as discussed in previous case of the twisted pair cable. Furthermore discrepancies are observed between Ey calculated by the current of MoM (figure 13) and the calculated by measured current in figure 15. Such errors can be ascribed to the fact the experimental termination box comprises parasitic capacitance and inductance, which is further complex than pure resistance of Table I in MoM Model. However, it does not influence the accuracy of proposed CASM because one advantage of this method is free from termination information.

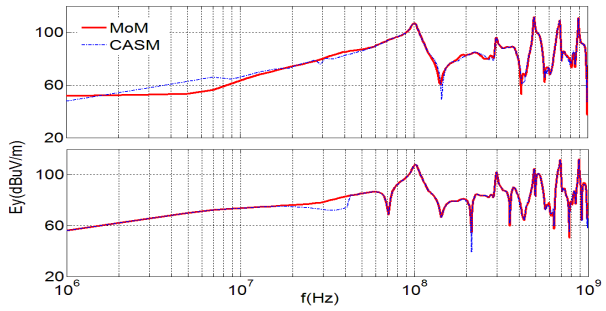

Figure 13. E_y at observation point by MoM and CASM for the fed cable with a low resistance (upper) and high resistance (lower)

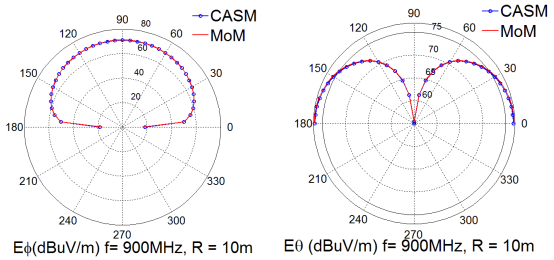

Figure 14. Far-field by MoM and CASM for fed cable with a low resistance

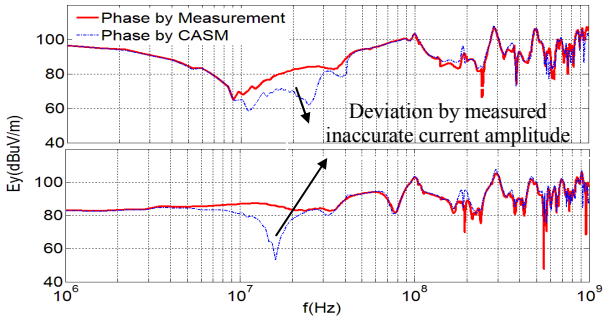

Figure 15. The calculated E_y when the phase is measured and retrieved by CASM for fed cable with a low resistance (upper) and high resistance (lower)

C. *A twisted pair cable driven by differential voltage pair*

In real EMC measurement spectrum analyzer is usually as receiving equipment. In order to verify the proposed CASM in this work, we still investigated the radiation from a twisted pair cable and measured the receive voltage on the rod antenna, as shown in figure 6. However in this model the twisted pair cable was fed by differential voltage pair with 2-port signal generator (figure 16). The differential voltage sources V_p and V_m are pluses with frequency 40 MHz and amplitude 2.5 V. The asymmetric delay time (V_m to V_p) is 5 ns, due to this reason there is a common mode voltage contribution V_{com} (V_p + V_m), as shown in figure 17.

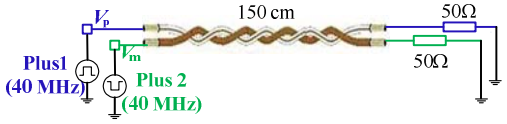

Figure 16. The tested cable driven by differential voltage pair

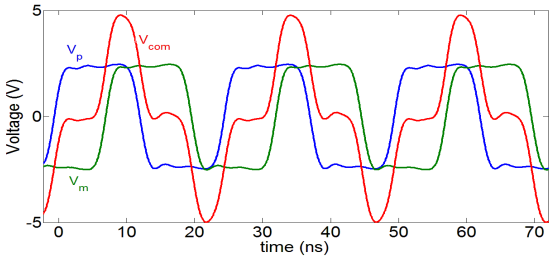

Figure 17. The differential voltage pair and common mode voltage

We first scanned the current amplitude at different points along the cable with a RF current probe and spectrum analyzer. Then we applied CASM to retrieve the phase information at each frequency; finally we combined multiple-dipole method (MDM) and mirror theory to calculate the electric field at observation point. In order to compare this prediction value, the measured antenna voltage is transformed to a field value through AF_{MoM} in (19). Figure 18 depicts the results of CASM and measurement from 30 MHz to 400 MHz. It can be seen from these two curves, the predicted values at frequencies of multiples of 40 MHz match well with measured data. The deviation below 320 MHz is less than or equal to 3 dB, while the deviations at 360 MHz and 400 MHz amount to 4.6 dB and 4.1 dB. This deviation might be due to main two reasons: Measured current amplitude and scanning position error and error of calculated rod antenna factor AF_{MoM}.

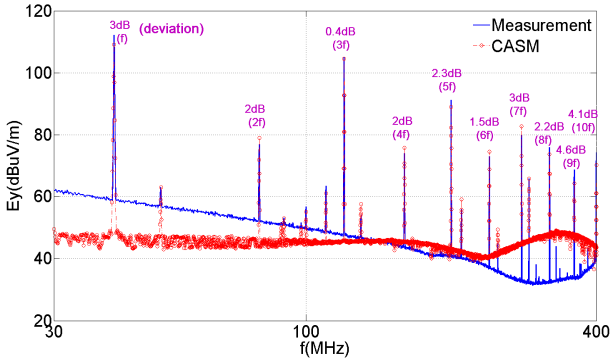

Figure 18. E_y at the observation point from measurement and CASM (fundamental frequency is 40 MHz)

V. CONCLUSION

This paper presents a novel approach to predict radiated emissions from a cable bundle. The needed phase information, based on measured amplitude of common mode current along a cable bundle, was retrieved by an optimization algorithm. With multi-dipole methods the electromagnetic fields are calculated. For retrieving the phase of common mode current along a cable bundle, TRR algorithm was introduced to find transmission line optimized parameters set $P(A, B, \alpha, \beta)$. To verify the proposed method this paper investigated radiation from a twisted pair cable, operated in common and differential mode, and a larger bundle model composed of seven cables with random terminations. The proposed method can accurately predict radiated fields only from knowledge of the measured common mode current amplitude from a cable bundle. However, in real measurement process scanning position and amplitude errors may lead to deviations of final prediction results at some frequencies. Here additional analysis is necessary. In low frequency range (below 30 MHz), CASM could fail predicting correct phase and radiated field. The reason for this failure is not understood completely and will be analyzed in future intensively.

The main motivation of the presented work is to develop a new measurement method, aiming at avoiding expensive anechoic chambers for component/modules radiation emissions measurements. Good accuracy, low costs, and less space consumption make this method promising for pre-compliance tests of automotive products.

REFERENCES

[1] CISPR 25 Ed.3, "Vehicles, boats and internal combustion engines-Radio disturbance characteristics – Limits and methods of measurements for the protection of on-board receivers", 2007

[2] W. T. Smith, K. Frazier, "Prediction of Anechoic Chamber Radiated Emissions Measurements through Use of Empirically-Derived Transfer Functions and Laboratory Common-Mode Current Measurements", *IEEE International Symposium on Electromagnetic Compatibility*, Aug. 1998.

[3] D. Rinas, S. Niedzwiedz, J. Jia, S. Frei, "Optimization methods for equivalent source identification and electromagnetic model creation based on near-field measurements", *EMC Europe* 2011, *York*, Sept. 2011, pp. 298-303.

[4] Y. Vives-Gilabert, C. Arcambel, A. Louis, F. De Daran, P. Eudeline, and B. Mazari, "Modeling magnetic radiation of electronic circuits using near-field scanning method", *IEEE Trans. Electromagn. Compat.,* vol.49, no.2, pp.391-400, May 2007.

[5] T. Isernia, G. Leone, R. Pierri, "Radiation pattern evaluation from near-field intensities on planes", *IEEE Trans. Antennas Propogat*., vol.44, pp.701-710, May 1996.

[6] C. R. Paul, "Analysis of Multiconductor Transmission Lines", New York: Wiley, 1997.

[7] C. Poudroux, M. Rifi, "A simplified approach to determine the amplitude of the transient voltage induced on a cable bundle", *IEEE Trans. Electromagn. Compat*., vol.37, no.4, pp.497-504, Nov. 1995.

[8] F. Grassi, G. Spadacini, F.Marliani, and S. A. Pignari, "Use of double bulk current injection for susceptibility testing of avionics", *IEEE Trans. Electromagn. Compat*., vol.50, no.3, pp.524-535, Aug . 2008.

[9] MATLAB, Help Handbook, "Solve nonlinear curve-fitting problems in least-squares" and "How GlobalSearch and MultiStart Work", 2010.

[10] J. Jia, F. Kremer, S. Frei, "Modellierung von CISPR-25 Antennenmessungen mittels schneller approximierender Berechnungsverfahren", *EMV-Düsseldorf*, *Germany*, 2012.